LETTERS
https://doi.org/10.1038/s41550-019-0880-2

nature astronomy

Relativistic Shapiro delay measurements of an extremely massive millisecond pulsar

H. T. Cromartie[1]*, E. Fonseca[2], S. M. Ransom[3], P. B. Demorest[4], Z. Arzoumanian[5], H. Blumer[6,7], P. R. Brook[6,7], M. E. DeCesar[8], T. Dolch[9], J. A. Ellis[10], R. D. Ferdman[11], E. C. Ferrara[12,13], N. Garver-Daniels[6,7], P. A. Gentile[6,7], M. L. Jones[6,7], M. T. Lam[6,7], D. R. Lorimer[6,7], R. S. Lynch[14], M. A. McLaughlin[6,7], C. Ng[15,16], D. J. Nice[8], T. T. Pennucci[17], R. Spiewak[18], I. H. Stairs[15], K. Stovall[4], J. K. Swiggum[19] and W. W. Zhu[20]

Despite its importance to our understanding of physics at supranuclear densities, the equation of state (EoS) of matter deep within neutron stars remains poorly understood. Millisecond pulsars (MSPs) are among the most useful astrophysical objects in the Universe for testing fundamental physics, and place some of the most stringent constraints on this high-density EoS. Pulsar timing—the process of accounting for every rotation of a pulsar over long time periods—can precisely measure a wide variety of physical phenomena, including those that allow the measurement of the masses of the components of a pulsar binary system[1]. One of these, called relativistic Shapiro delay[2], can yield precise masses for both an MSP and its companion; however, it is only easily observed in a small subset of high-precision, highly inclined (nearly edge-on) binary pulsar systems. By combining data from the North American Nanohertz Observatory for Gravitational Waves (NANOGrav) 12.5-yr data set with recent orbital-phase-specific observations using the Green Bank Telescope, we have measured the mass of the MSP J0740+6620 to be $2.14^{+0.10}_{-0.09}\,M_\odot$ (68.3% credibility interval; the 95.4% credibility interval is $2.14^{+0.20}_{-0.18}\,M_\odot$). It is highly likely to be the most massive neutron star yet observed, and serves as a strong constraint on the neutron star interior EoS.

Relativistic Shapiro delay, which is observable when a pulsar passes behind its stellar companion during orbital conjunction, manifests as a small delay in pulse arrival times induced by the curvature of spacetime in the vicinity of the companion star. For a highly inclined MSP–white dwarf binary, the full delay is on the order of ~10 μs. The relativistic effect is characterized by two parameters, 'shape' and 'range'. In general relativity, shape (s) is the sine of the angle of inclination of the binary orbit (i), while range (r) is proportional to the mass of the companion, m_c. When combined with the Keplerian mass function, measurements of r and s also constrain the pulsar mass (m_p; ref. [3] provides a detailed overview and an alternative parameterization).

Precise neutron star mass measurements are an effective way to constrain the EoS of the ultradense matter in neutron star interiors. Although radio pulsar timing cannot directly determine neutron star radii, the existence of pulsars with masses exceeding the maximum mass allowed by a given model can straightforwardly rule out that EoS.

In 2010, Demorest et al. reported the discovery of a $2\,M_\odot$ MSP, J1614−2230 (ref. [4]) (though the originally reported mass was $1.97 \pm 0.04\,M_\odot$, continued timing has led to a more precise mass measurement of $1.928 \pm 0.017\,M_\odot$ by Fonseca et al.[5]). This Shapiro-delay-enabled measurement disproved the plausibility of some hyperon, boson and free quark models in nuclear-density environments. In 2013, Antoniadis et al. used optical techniques in combination with pulsar timing to yield a mass measurement of $2.01 \pm 0.04\,M_\odot$ for the pulsar J0348+0432 (ref. [6]). These two observational results (along with others[7]) encouraged a reconsideration of the canonical $1.4\,M_\odot$ neutron star. Gravitational-wave astrophysics has also begun to provide EoS constraints; for example, the Laser Interferometer Gravitational-Wave Observatory (LIGO) detection of a double neutron star merger constrains permissible EoSs, suggesting that the upper limit on neutron star mass is $2.17\,M_\odot$ (90% credibility[8]). Though the existence of extremely massive ($>2.4\,M_\odot$) neutron stars has been suggested through optical spectroscopic and photometric observations (for example ref. [9]), radio timing can provide much more precise constraints on the existence of $\gtrsim 2\,M_\odot$ neutron stars.

NANOGrav employs pulsar timing for an important general relativistic application: the detection of low-frequency gravitational waves primarily from supermassive black hole binaries. The collaboration's observing programme consists of high-cadence, multifrequency radio observations of ~75 MSPs using the Green Bank and Arecibo telescopes (GBT and AO; see ref. [10] and the upcoming 12.5-yr data release). Additionally, NANOGrav has begun using the Karl G. Jansky Very Large Array as the third

---

[1]Department of Astronomy, University of Virginia, Charlottesville, VA, USA. [2]Department of Physics, McGill University, Montreal, QC, Canada. [3]National Radio Astronomy Observatory, Charlottesville, VA, USA. [4]National Radio Astronomy Observatory, Socorro, NM, USA. [5]X-ray Astrophysics Laboratory, Code 662, NASA Goddard Space Flight Center, Greenbelt, MD, USA. [6]Department of Physics and Astronomy, West Virginia University, Morgantown, WV, USA. [7]Center for Gravitational Waves and Cosmology, West Virginia University, Morgantown, WV, USA. [8]Department of Physics, Lafayette College, Easton, PA, USA. [9]Department of Physics, Hillsdale College, Hillsdale, MI, USA. [10]Infinia ML, Durham, NC, USA. [11]School of Chemistry, University of East Anglia, Norwich, UK. [12]NASA Goddard Space Flight Center, Greenbelt, MD, USA. [13]Department of Astronomy, University of Maryland, College Park, MD, USA. [14]Green Bank Observatory, Green Bank, WV, USA. [15]Department of Physics and Astronomy, University of British Columbia, Vancouver, BC, Canada. [16]Dunlap Institute, University of Toronto, Toronto, ON, Canada. [17]Hungarian Academy of Sciences MTA-ELTE 'Extragalactic Astrophysics Research Group', Institute of Physics, Eötvös Loránd University, Budapest, Hungary. [18]Centre for Astrophysics and Supercomputing, Swinburne University of Technology, Hawthorn, VIC, Australia. [19]Center for Gravitation, Cosmology and Astrophysics, Department of Physics, University of Wisconsin—Milwaukee, Milwaukee, WI, USA. [20]CAS Key Laboratory of FAST, NAOC, Chinese Academy of Sciences, Beijing, China. *e-mail: thankful@virginia.edu

observatory in its pulsar-timing programme. Using the GBT, NANOGrav regularly observes J1614−2230 and another high-mass radio MSP, J0740+6620.

PSR J0740+6620 (period = 2.89 ms) was discovered in the Green Bank Northern Celestial Cap 350 MHz survey (GBNCC) in 2012 (ref. [11]). It is in a nearly circular (eccentricity = 5×10^{-6}), 4.77-day orbit (Lynch et al. presented a recent GBNCC timing solution in 2018; ref. [12]). Recent optical and near-infrared observations by Beronya et al. (2019) revealed that its companion is probably the coolest white dwarf ever measured in orbit with an MSP[13].

Here we present timing observations of the pulsar with the GBT taken between 2014 and 2019. We observed the pulsar regularly throughout this period as part of the NANOGrav timing programme[10]. This section of our data set includes ~70 epochs (occurring approximately monthly and at random orbital phases) during which the pulsar was observed at both 1.4 GHz and 820 MHz for ~20 min each. We were awarded additional time for two concentrated campaigns over superior conjunction (that is, when the pulsar is behind its companion star), as probing the minima and maxima of the Shapiro delay signal is the best way to improve the signal's detectability (see the absorbed or 'detectable' signal in the second panel of Fig. 1).

After the second concentrated campaign consisting of two 5 h observations at orbital phases 0.15 and 0.25 (GBT 18B-372), the timing analysis (see details in Methods) yielded a pulsar mass of $2.14^{+0.10}_{-0.09}\,M_{\odot}$ at 68.3% credibility (Fig. 2). Methods describes our rationale for choosing these two orbital phases, as well as the progression of mass measurements and precisions as more observations were added. Our final fits with and without Shapiro delay as a function of orbital phase are presented in Fig. 1, and the top panel of Fig. 3 shows timing residuals spanning the entire data set. Although our measured relative uncertainty is higher than, for example, the original relative error reported by Demorest et al. for J1614−2230 (5% versus 2%), J0740+6620 is a remarkably high-mass MSP. This measurement will help constrain high-density nuclear physics, as there are very few examples of $\gtrsim 2\,M_{\odot}$ neutron stars. PSR J0740+6620 is 98% and 90% likely to be more massive than J1614−2230 and J0348+0432, respectively, and is therefore likely to be the most massive well measured neutron star so far.

Taken together, these three massive MSPs serve as a strong validation of the existence of high-mass neutron stars. Due to the asymptotic nature of the relationship between maximum neutron star mass and nearly all EoSs, even small increases in the measured mass of the most massive neutron stars force a reconsideration of the fundamental physics at play in their interiors (for example, see Fig. 2 in ref. [14]). Non-nucleonic solutions to the EoS problem, such as quark matter, hyperons or Bose–Einstein meson condensates, yield softer EoSs (that is, relatively compressible matter); however, more massive neutron stars necessitate stiffer EoSs, which allow for higher maximum masses (see ref. [15] for a review). The measurement of a $2.14\,M_{\odot}$ neutron star is therefore in extreme tension with these non-nucleonic proposals, and underlines the necessity of untangling existing theoretical paradoxes. The most prominent of these may be the hyperon problem, which proposes that, although the extreme densities inside neutron stars would favour the conversion of nucleons to hyperons, the presence of hyperons softens the EoS and excludes the possibility of high-mass neutron stars (see, for example, ref. [16]). In addition, the mass measurement of J0740+6620 may have implications for the nature of neutron star mergers as detected by LIGO. Because several neutron stars with masses close to or greater than $\sim 2\,M_{\odot}$ are now known, it may be the case that more mass-asymmetric neutron star mergers will occur than previously supposed.

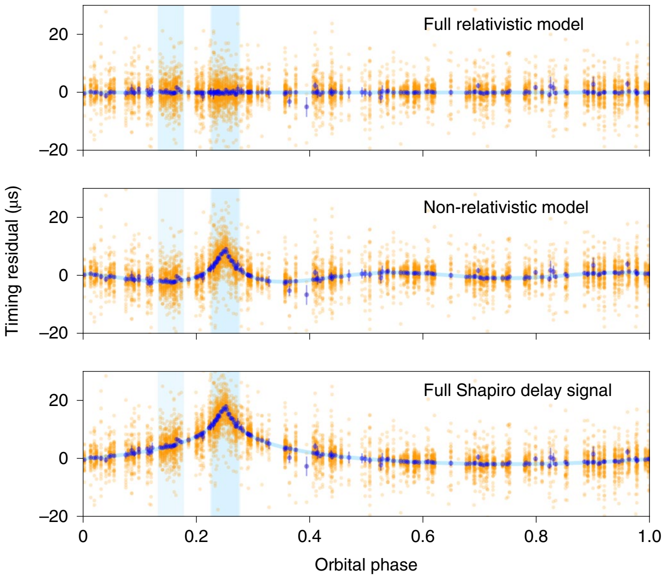

Fig. 1 | Timing residuals from all observations of J0740+6620 as a function of orbital phase, with superior conjunction at orbital phase = 0.25. Orange points are multifrequency timing residuals, while dark-blue points are averages of each group (timing epoch) of these points with 1σ error bars. Averages were taken over a minimum of four data points to avoid showing misleading residuals from faint observations. Blue boxes indicate the orbital phases over which each of the three supplemental observations was taken (the box over conjunction is slightly darker because we made two superior conjunction observations). The top panel shows the full fit (including Shapiro delay parameters and all dispersion measure (DM) parameters—that is, the full timing solution). The middle panel is the best fit with the measurable Shapiro delay signal added; this is the signal to which we are actually sensitive. The bottom panel is the 'full' Shapiro delay signal. Both the second and third panels are calculated on the basis of the orbital and system parameters determined from the full fit. The lighter-blue line represents the theoretical measurable and full Shapiro delay in the middle and bottom panels, respectively (and marks a 0 μs residual in the top panel). The width of the line in each panel is equal to the root mean square error of the averaged points.

Constraining the mass of J0740+6620 carries additional astrophysical benefits. Recent evidence from Antoniadis et al.[17] suggests that the distribution of MSP masses may be bimodal, implying that many more neutron stars with masses greater than $\sim 1.6\,M_{\odot}$ may exist than previously supposed (see also ref. [15]). Not only is it becoming clear that high-mass neutron stars make up a sizeable portion of the population, but also their existence carries substantial implications for our understanding of MSP binary evolution. Because many fully recycled pulsars have been measured to have masses less than or equal to $1.4\,M_{\odot}$, we know that recycling can be accomplished with only a small amount of mass transfer. We must therefore consider the possibility that some MSPs are not formed near the Chandrasekhar mass and increase to high masses through accretion; rather, they are born massive in the first place (see refs. [18] and [19] for earlier evidence of this phenomenon).

There exists a well known relationship between the mass of a pulsar's white dwarf companion and the binary system's orbital period[20,21]. For our measured orbital period of ~4.77 days, the predicted white dwarf companion masses (from equations (20) and (21) in ref. [21]) are $\sim 0.24\,M_{\odot}$ for a mid-metallicity (Pop I+II) donor star and $\sim 0.25\,M_{\odot}$ for a low-metallicity, Pop II star. Our measured mass of J0740+6620's helium white dwarf companion is $0.260^{+0.008}_{-0.007}\,M_{\odot}$ (at 68.3% credibility). Given the stated uncertainties in convective mixing length, this discrepancy of 5–10% is not an indication that J0740+6620 is an exception to the orbital period versus white dwarf mass relationship; however, it may indicate that this system was born in a relatively low-metallicity environment. There exist

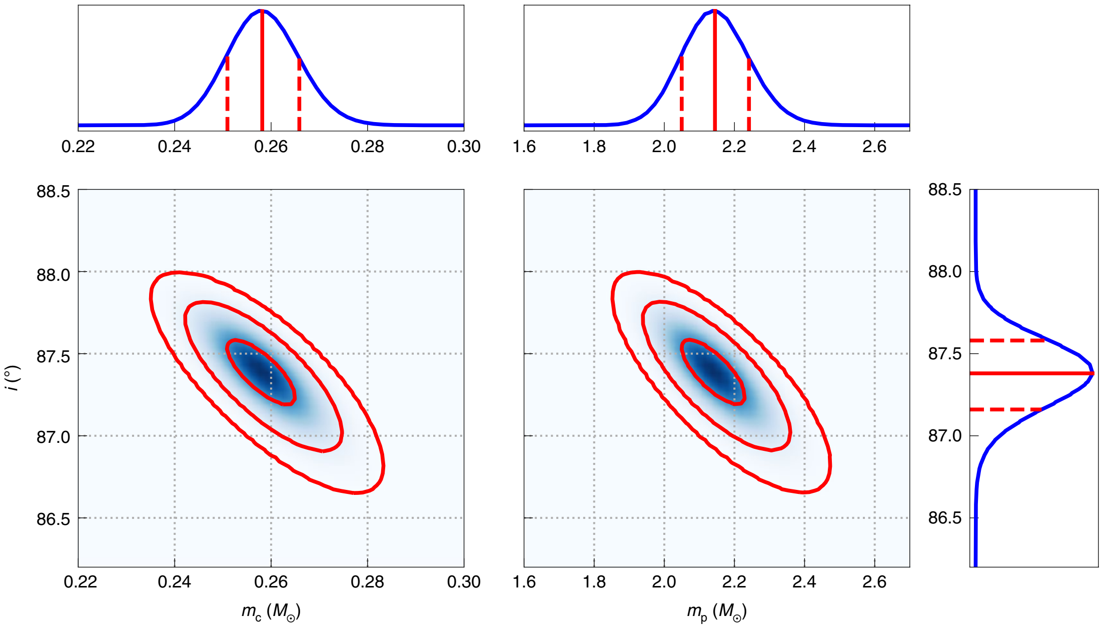

Fig. 2 | Map of fitted χ^2 distributions and corresponding probability density functions for m_p, m_c and i. The left-hand heat map was generated by computing χ^2 values for different combinations of m_c and i; the right-hand heat map was calculated by translating the m_c–i probability density function to the m_p–i phase space using the binary mass function. Darker-blue regions correspond to lower χ^2 values. The three red circles correspond to 1, 2 and 3σ significance cut-offs. Each of the three probability density functions (blue lines plotted above and beside the heat maps) is a projection of the χ^2 distributions. The solid red lines mark median values of each of the three parameters, while red dashed lines denote the upper and lower bounds of the 68.3% (1σ) credibility interval.

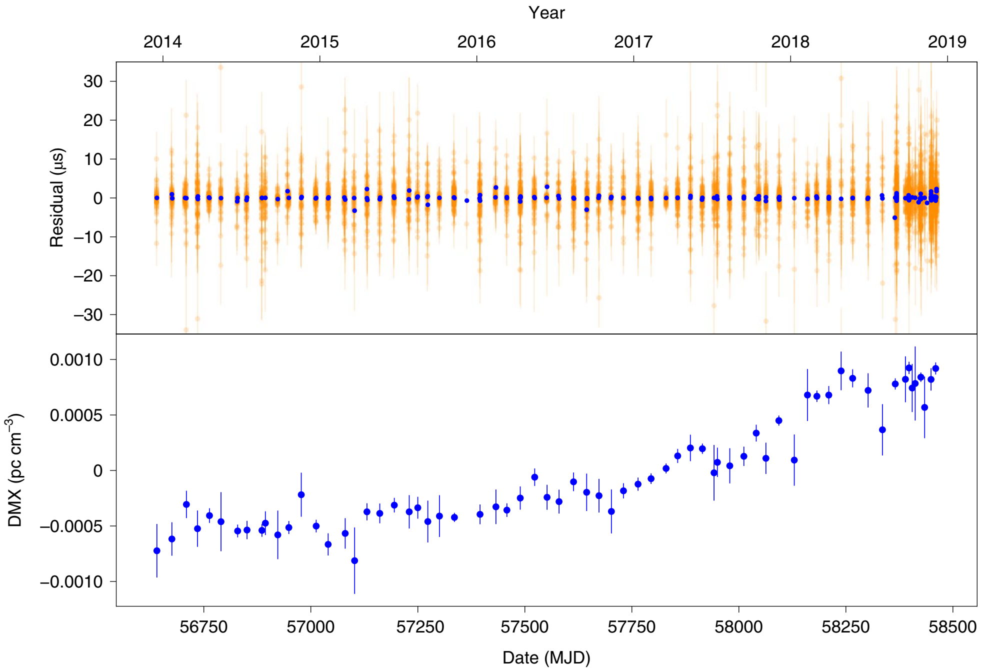

Fig. 3 | Timing residuals and DMX for all epochs of J0740+6620 data. Top: timing residuals from all epochs of J0740+6620 data, including both NANOGrav and superior conjunction-specific observations at all frequencies, are shown in orange (with 1σ error bars). The superimposed blue points represent an average over each epoch (root mean square = 1.5 μs; note that some days have two separately calculated averages from dual-frequency data). Bottom: blue points indicate DMX values calculated for each epoch of data with 1σ error bars, where DMX is a piecewise constant approximation to the DM. The DMX trend is fairly simple (that is, roughly quadratic); however, linear modelling is strongly disfavoured. A single averaged epoch (one dark-blue point) was removed from these plots, as its error bar was ~8 μs due to a faint detection from which only one time of arrival (TOA) could be extracted. MJD, modified Julian date.

at least three other examples of MSP–helium white dwarf binaries with minimum companion masses greater than the Pop II masses predicted by Tauris and Savonije (J1125−6014, J1903−7051 and J1933−6211). Finally, if J0740+6620 is measured to be at the high end of our mass credibility interval, it may provide evidence that the creation of a stable, high-mass neutron star is possible through the merger of two low-mass neutron stars (in a LIGO-like gravitational-wave event).

Though it will require considerable additional observing time to improve on our J0740+6620 measurement, high-cadence monitoring of the pulsar is a promising strategy. Daily observations with the Canadian Hydrogen Intensity Mapping Experiment (CHIME[22]) telescope, in conjunction with the present data set, have the potential to determine the mass of J0740+6620 with 2–3% precision within a year. Additionally, the Neutron Star Interior Composition Explorer (NICER) is observing J0740+6620 at X-ray wavelengths (https://heasarc.gsfc.nasa.gov/docs/nicer/science_team_investigations). Modelling the thermal pulse profile of this MSP at X-ray energies will aid in constraining the mass and radius of J0740+6620. Continued collaboration with multifrequency observing programmes will guarantee the steady improvement of this pulsar mass measurement in the long term.

Methods

GBT observations. Both NANOGrav and targeted observations were conducted using the Green Bank Ultimate Pulsar Processing Instrument (GUPPI[23]). Observations at 1.5 GHz were acquired with 800 MHz of bandwidth split into 512 frequency channels (which were summed to 64 channels before analysis), sampling every 0.64 μs. At an observing frequency of 820 MHz, 200 MHz of bandwidth over 128 channels was acquired with an identical sampling rate (and later also summed to 64 channels). These dual-polarization observations at both frequencies were coherently dedispersed at the known DM of 15.0 pc cm^{-3}. Data were processed using NANOGrav pipelines for consistency with the existing 4-yr-long NANOGrav J0740+6620 data set (see ref. [24] for a thorough description of NANOGrav observing procedures, and ref. [25] for a description of NANOGrav's main data processing pipeline, `nanopipe`).

Generation of TOAs and the timing model. The measurement and modelling of pulse TOAs closely mirrors the procedure described by Arzoumanian et al.[10]. We provide a summary of the analysis procedure in this section.

During offline processing, total-intensity profile data were integrated over ~20–30 min intervals to yield one or two TOAs per downsampled frequency interval for a normal NANOGrav observation, and ~10 min for the long scans near or during conjunction. We extracted TOAs from each of the 64 integrated channels over the entire observing bandwidth through cross-correlation between the data and a smoothed profile template using the software package `PSRCHIVE` (source code in ref. [26]; see http://psrchive.sourceforge.net).

We used standard pulsar-timing analysis tools, namely `TEMPO` (http://tempo.sourceforge.net) and `TEMPO2` (source code in ref. [27]; see https://www.atnf.csiro.au/research/pulsar/tempo2) for modelling TOA variation in terms of many physical mechanisms. `TEMPO` and `TEMPO2`, while not fully independent timing packages, yield consistent results. For J0740+6620, fitted parameters include celestial (ecliptic) coordinates, proper motion, spin frequency and its first derivative, and binary orbital parameters (see Table 1, which lists best-fit values for these parameters as determined with `TEMPO`).

We used the DE436 (https://naif.jpl.nasa.gov/pub/naif/JUNO/kernels/spk/de436s.bsp.lbl) Solar System ephemeris, maintained by the NASA Jet Propulsion Laboratory, for correction to the barycentric reference frame. The time standard used was BIPM2017. The overall root mean square timing residual value for the timing model presented in this work is 1.5 μs. The χ^2 of our fit is 7,314.35 with 7,334 degrees of freedom, yielding a reduced-χ^2 value of 0.997; note that the noise modelling (Assessment of timing noise) will always yield a χ^2 of ~1.

We employed the ELL1 binary timing model[28] in describing the nearly circular orbital dynamics of the J0740+6620 system. Parameters of the ELL1 binary model consist of the projected semi-major axis, orbital period, epoch of passage through the ascending orbital node, and two 'Laplace–Lagrange parameters' (ϵ_1 and ϵ_2; the orbital eccentricity multiplied by the sine and cosine of periastron longitude, respectively[28]) that quantify departures from perfectly circular orbits.

Assessment of timing noise. MSP rotation often exhibits a limit in achievable precision due to the presence of stochastic processes that act as noise in timing measurements. Examples of timing noise include systematic errors from cross-correlation template matching and 'spin noise' due to irregular rotation of the neutron star. We use a noise model similar to those developed in the NANOGrav 9-yr and 11-yr data releases to quantify these noise terms in the J0740+6620 data set.

The noise model consists of white-noise components that combine to form additive Gaussian noise. For each of the two front-end receivers used in this work, we use three parameters to describe the white-noise contribution to timing noise: a scaling factor applied to all raw TOA uncertainties ('EFAC'), a term added in quadrature to the TOA uncertainties ('EQUAD') and a noise term that quantifies TOA correlations purely across observing frequency ('ECORR').

Table 1 | PSR J0740+6620 best-fit parameters

Pulsar name	J0740+6620
Dates of observations (MJD)	56640–58462
Number of TOAs	7,419
Measured quantities	
Ecliptic longitude, λ (°)	103.75913607(1)
Ecliptic latitude, β (°)	44.10248468(2)
Epoch of position and period (MJD)	57551.0
Proper motion in ecliptic longitude (mas yr^{-1})	−2.75(3)
Proper motion in ecliptic latitude (mas yr^{-1})	−32.43(4)
Parallax (mas)	0.5(3)
Spin frequency, ν (Hz)	346.5319964932129(6)
Spin frequency derivative, $\dot{\nu}$ (s^{-2})	$-1.46389(2)\times10^{-15}$
Dispersion measure, DM (pc cm^{-3})[a]	14.961787
Profile frequency dependency parameter, FD1	$-1.17(4)\times10^{-5}$
Binary model	ELL1
Projected semi-major axis of orbit, x (lt-s)	3.9775561(2)
Binary orbital period, P_b (days)	4.7669446191(1)
Epoch of ascending node, TASC (MJD)	57552.08324415(2)
EPS1 (first Laplace–Lagrange parameter), $e\sin\omega$	$-5.70(4)\times10^{-6}$
EPS2 (second Laplace–Lagrange parameter), $e\cos\omega$	$-1.89(3)\times10^{-6}$
Sine of inclination angle i	0.9990(2)
Companion mass, m_c ($M_\odot$)	0.258(8)
Derived parameters	
Orbital eccentricity, e	$5.10(3)\times10^{-6}$
Longitude of periastron, ω (°)	244.4(3)
Epoch of periastron, T_0 (MJD)	57550.543(5)
Binary mass function ($M_\odot$)	0.0029733870(4)
Pulsar mass (68.3% credibility interval, $M_\odot$)	$2.14^{+0.10}_{-0.09}$
Pulsar mass (95.4% credibility interval, $M_\odot$)	$2.14^{+0.20}_{-0.18}$
Companion mass (68.3% credibility interval, $M_\odot$)	$0.260^{+0.008}_{-0.007}$
Companion mass (95.4% credibility interval, $M_\odot$)	$0.260^{+0.016}_{-0.014}$
Inclination angle (68.3% credibility interval, °)	$87.38^{+0.20}_{-0.22}$
Inclination angle (95.4% credibility interval, °)	$87.38^{+0.39}_{-0.45}$

[a] Because this DM is an unfitted reference value, no error is reported. Values of DMX for each of the ~70 epochs are available on request.

We used the `Enterprise` (https://enterprise.readthedocs.io/en/latest) modelling suite for estimation of the white components of the noise model using a Markov chain Monte Carlo (MCMC)-based algorithm. `Enterprise` uses the `TEMPO(2)` fit as the maximum-likelihood fit for the timing parameters and the basis of the fit for the red-noise parameters, should they be found to be significant. In our `TEMPO(2)` fits, we include an EFAC of 1.036 for L-band (1,500 MHz) TOAs and 1.013 for 820 MHz TOAs. EQUAD is 0.00610 μs for the L band, and 0.18310 μs for 820 MHz. ECORR values for L-band and 820 MHz TOAs are 0.00511 μs and 0.00871 μs, respectively. Bayesian model selection via an `Enterprise` MCMC run disfavours the inclusion of red noise; therefore, the noise model includes only white-noise components.

DM modelling. The complexity of modelling DM variations arising from a dynamic interstellar medium has been discussed at length in previous works (see, for example, refs. [29,30]). We have adopted the standard NANOGrav piecewise-constant model for DM trends wherein each epoch of data is fitted with a constant DMX value; in other words, each of these parameters is a deviation from some nominal DM and is fixed over a single epoch. The observation that J0740+6620's DM behaviour is fairly smooth over the duration of our data set (see Fig. 3) led us to attempt alternatively modelling the entire data set by fitting for only the first and second derivatives of DM. In theory, this approach could be advantageous given the ability of DMX to absorb Shapiro delay signals (thanks to the similar duration of conjunction and a DMX epoch). While this strategy does reduce the formal parameter uncertainties from the fit, both an F-test and an Akaike information criterion test strongly favour the DMX model over the quadratic DM fit. This indicates that the DM variation is not fully characterized by a quadratic model, and parameter values (including pulsar mass) derived from this model are likely to have systematic biases not reflected in their formal uncertainties.

Simulations. Analysis of the NANOGrav 12.5-yr data set without supplemental data yielded $m_{\rm p} = 2.00 \pm 0.20\,M_{\odot}$. After the initial 6 h supplemental observation, we measured the mass of J0740+6620 to be $2.18 \pm 0.15\,M_{\odot}$. We conducted simulations of future observations both to predict the constraining power of a concentrated Director's Discretionary Time campaign and to determine how our mass measurement may improve with additional observations going forward. For these simulations, we first generated an arbitrary array of TOAs that mirror the desired observing cadence, starting date and so on. The TOAs were then fitted (with pulsar-timing software such as `TEMPO` or `PINT`; https://github.com/nanograv/PINT) using the known parameters for J0740+6620. Residuals from this fit were then subtracted from the original TOAs to create 'perfect' TOAs, to which stochastic noise was then added. Two notable types of simulation were conducted. The first was an estimation of the improvement in our measurement of $m_{\rm p}$ given random orbital sampling (the 'NANOGrav-only observation' scenario); this solidified our conclusion that the concentrated GBT campaigns were necessary. The second served to optimize our observing strategy during a targeted orbital-phase campaign by trying various permutations of orbital phase, number of observing sessions and observing session lengths. The results of this simulation informed our GBT Director's Discretionary Time request for 5 h over conjunction and 5 h in one of the Shapiro 'troughs' (we were awarded time in the first trough—around orbital phase 0.15—in addition to conjunction). To ensure that obtaining data in this asymmetric fashion would not bias our mass measurement, we ran 10,000 simulations of a 5 h conjunction observation plus 5 h in either the first or second Shapiro trough. The averages of the 10,000 mass measurements obtained from each of these troughs were consistent within 1%, implying that our orbital sampling is not biasing our results (as one would expect, given that the Shapiro delay response curve is symmetric about superior conjunction).

Data availability

PSR J0740+6620 TOAs from both the 12.5-yr data set and from the two supplemental GBT observations will be available at https://data.nanograv.org on publication of this manuscript.

Code availability

All code mentioned in this work is open source and available at the links provided in the manuscript.

Received: 13 April 2019; Accepted: 31 July 2019;
Published online: 16 September 2019

References

1. Lorimer, D. R. & Kramer, M. *Handbook of Pulsar Astronomy* (Cambridge University Press, 2005).
2. Shapiro, I. I. Fourth test of general relativity. *Phys. Rev. Lett.* **13**, 789–791 (1964).
3. Freire, P. C. C. & Wex, N. The orthometric parametrization of the Shapiro delay and an improved test of general relativity with binary pulsars. *Mon. Not. R. Astron. Soc.* **409**, 199–212 (2010).
4. Demorest, P. B., Pennucci, T., Ransom, S. M., Roberts, M. S. E. & Hessels, J. W. T. A two-solar-mass neutron star measured using Shapiro delay. *Nature* **467**, 1081–1083 (2010).
5. Fonseca, E. et al. The NANOGrav nine-year data set: mass and geometric measurements of binary millisecond pulsars. *Astrophys. J.* **832**, 167 (2016).
6. Antoniadis, J. et al. A massive pulsar in a compact relativistic binary. *Science* **340**, 448 (2013).
7. Friere, P. C. C. et al. On the nature and evolution of the unique binary pulsar J1903+0327. *Mon. Not. R. Astron. Soc.* **412**, 2763–2780 (2011).
8. Margalit, B. & Metzger, B. D. Constraining the maximum mass of neutron stars from multi-messenger observations of GW170817. *Astrophys. J. Lett.* **850**, L19 (2017).
9. Linares, M., Shahbaz, T. & Casares, J. Peering into the dark side: magnesium lines establish a massive neutron star in PSR J2215+5135. *Astrophys. J.* **859**, 54 (2018).
10. Arzoumanian, Z. et al. The NANOGrav 11-year data set: pulsar-timing constraints on the stochastic gravitational-wave background. *Astrophys. J.* **859**, 47 (2018).
11. Stovall, K. et al. The Green Bank Northern Celestial Cap pulsar survey. I. Survey description, data analysis, and initial results. *Astrophys. J.* **791**, 67 (2014).
12. Lynch, R. S. et al. The Green Bank North Celestial Cap pulsar survey. III. 45 new pulsar timing solutions. *Astrophys. J.* **859**, 93 (2018).
13. Beronya, D. M. et al. The ultracool helium-atmosphere white dwarf companion of PSR J0740+6620?. *Mon. Not. R. Astron. Soc.* **485**, 3715–3720 (2019).
14. Watts, A. et al. Probing the neutron star interior and the Equation of State of cold dense matter with the SKA. *Proc. Sci.* **215**, 43 (2015).
15. Özel, F. & Freire, P. Masses, radii, and the equation of state of neutron stars. *Annu. Rev. Astron. Astrophys.* **54**, 401–440 (2016).
16. Bedaque, P. F. & Steiner, A. W. Hypernuclei and the hyperon problem in neutron stars. *Phys. Rev. C* **92**, 025803 (2015).
17. Antoniadis, J. et al. The millisecond pulsar mass distribution: Evidence for bimodality and constraints on the maximum neutron star mass. Preprint at https://arxiv.org/abs/1605.01665 (2016).
18. Tauris, T. M., Langer, N. & Kramer, M. Formation of millisecond pulsars with CO white dwarf companions—I. PSR J1614-2230: evidence for a neutron star born massive. *Mon. Not. R. Astron. Soc.* **416**, 2130–2142 (2011).
19. Cognard, I. et al. A massive-born neutron star with a massive white dwarf companion. *Astrophys. J.* **844**, 128 (2017).
20. Rappaport, S., Podsiadlowski, P., Joss, P. C., Di Stefano, R. & Han, Z. The relation between white dwarf mass and orbital period in wide binary radio pulsars. *Mon. Not. R. Astron. Soc.* **273**, 731–741 (1995).
21. Tauris, T. M. & Savonije, G. J. Formation of millisecond pulsars. I. Evolution of low-mass X-ray binaries with $P_{\rm orb} > 2$ days. *Astron. Astrophys.* **350**, 928–944 (1999).
22. Ng, C. Pulsar science with the CHIME telescope. In *Proc. International Astronomical Union Vol. 13, Symp. 337: Pulsar Astrophysics —The Next Fifty Years* (eds Weltevrede, P. et al.) 179–182 (Cambridge University Press, 2018).
23. DuPlain, R. et al. Launching GUPPI: the Green Bank Ultimate Pulsar Processing Instrument. *Proc. SPIE* **7019**, 70191D (2008).
24. Arzoumanian, Z. et al. The NANOGrav nine-year data set: observations, arrival time measurements, and analysis of 37 millisecond pulsars. *Astrophys. J.* **813**, 65 (2015).
25. Demorest, P. B. nanopipe: calibration and data reduction pipeline for pulsar timing. *Astrophysics Source Code Library* ascl:1803.004 (2018).
26. van Straten, W. et al. PSRCHIVE: development library for the analysis of pulsar astronomical data. *Astrophysics Source Code Library* ascl:1105.014 (2011).
27. Hobbs, G. & Edwards, R. Tempo2: pulsar timing package. *Astrophysics Source Code Library* ascl:1210.015 (2012).
28. Lange, Ch et al. Precision timing measurements of PSR J1012+5307. *Mon. Not. R. Astron. Soc.* **326**, 274–282 (2001).
29. Lam, M. T. et al. Systematic and stochastic variations in pulsar dispersion measures. *Astrophys. J.* **821**, 66 (2015).
30. Jones, M. L. et al. The NANOGrav nine-year data set: measurement and interpretation of variations in dispersion measures. *Astrophys. J.* **841**, 125 (2017).

Acknowledgements

The NANOGrav Project receives support from NSF Physics Frontiers Center award no. 1430284. Pulsar research at UBC is supported by an NSERC Discovery Grant and by the Canadian Institute for Advanced Research (CIFAR). The National Radio Astronomy Observatory and the Green Bank Observatory are facilities of the National Science Foundation operated under cooperative agreement by Associated Universities, Inc. S.M.R is a CIFAR Senior Fellow. W.W.Z. is supported by the CAS Pioneer Hundred Talents Program, the Strategic Priority Research Program of the Chinese Academy of Sciences grant no. XDB23000000 and the National Natural Science Foundation of China grant nos. 11690024, 11743002 and 11873067. Supplementary Green Bank conjunction-phase observing project codes were 18B-289 and 18B-372 (DDT).

Author contributions

The creation of the NANOGrav 12.5-yr data set was made possible through extensive observations and pulsar-timing activities conducted by all the authors. H.T.C. was responsible for the NANOGrav-adjacent concentrated observing campaigns and the majority of this manuscript's contents. H.T.C., E.F., S.M.R. and P.B.D. were responsible for the extended J0740+6620 data analysis (the merging of NANOGrav and conjunction-phase observations) and modelling effort. E.F. was responsible for much of the initial work on J0740+6620 that informed the supplementary observing proposals, and for the development of the gridding code that yielded both the mass and inclination credibility intervals and Fig. 2.

Competing interests

The authors declare no competing interests.

Additional information

Reprints and permissions information is available at www.nature.com/reprints.

Correspondence and requests for materials should be addressed to H.T.C.

Peer review information *Nature Astronomy* thanks John Antoniadis and the other, anonymous, reviewer(s) for their contribution to the peer review of this work.